# Lorentz Levitation Technology: a New Approach to Fine Motion Robotics, Teleoperation, Haptic Interfaces, and Vibration Isolation

R. L. Hollis

IBM Research Division

T. J. Watson Research Center

Yorktown Heights, NY 10598, USA

S. E. Salcudean

Dept. of Electrical Engineering

University of British Columbia

Vancouver, BC, V6T 1Z4, Canada

## Abstract

*Recently, a new technology for stably levitating and controlling the position and orientation of a rigid body has been introduced. A unique feature is the use of Lorentz forces rather than the usual Maxwell forces as in magnetic bearings. The Lorentz force approach, which uses the force experienced by a conductor in a magnetic field, is seen to have several advantages. After an initial exploration phase and period of feasibility study, a number of potentially important applications are emerging. Among them are a way to provide fine compliant motion for assembly, to provide high fidelity force/torque feedback for teleoperation and virtual reality haptic interfaces, and to isolate sensitive payloads from environmental vibrational disturbances, either in space or on earth. In this paper we will discuss recent work intended to demonstrate the efficacy of Lorentz levitation technology for these application areas.*

## 1  Introduction

It has long been a dream to defy gravity and freely suspend a body in space, controlling it in all six degrees of freedom to perform some useful function. Whether flights of fancy or solid engineering achievements, many applications of such a capability have been envisioned over the years. Indeed, in limited fashion, both electric or magnetic methods have been used successfully for floating elements in devices such as electrostatic gyroscopes and magnetic bearings. Accordingly, unlike in ordinary mechanisms, there is an absence of separate moving parts for each degree of freedom and the attendant static friction, wear, and other deleterious dynamic effects.

We will not discuss electric methods here, but instead will focus on magnetic methods.

### 1.1  Survey of magnetic methods

In a long 1988 survey article Jayawant [1] listed the known technologies for magnetic levitation:

(i)  *repulsion between magnets of fixed strength;*

(ii)  *levitation by forces of repulsion and diamagnetic materials;*

(iii)  *levitation with superconducting magnets or superconducting surfaces;*

(iv)  *levitation by repulsion forces due to eddy currents induced in a conducting surface or body principally at power frequencies;*

(v)  *levitation by force acting on a current-carrying linear conductor in a magnetic field;*

(vi)  *suspension by a tuned* LCR *circuit and electrostatic force of attraction (between two plates);*

(vii)  *suspension by a tuned* LCR *circuit and magnetic force of attraction between an electromagnet and a ferromagnetic body;*

(viii)  *suspension by controlled* DC *electromagnets and the force of attraction between magnetized bodies;*

(ix)  *mixed μ system.*

Jayawant distinguishes between *suspension* where forces of attraction are used and *levitation* where the forces are repulsive. Techniques *(i)—(ix)* are examined below.

Earnshaw [2] proved in 1842 that a Newtonian field cannot possess stable points of equilibrium—only saddle points. Since a static electric or magnetic field is Newtonian, it follows that the technique *(i)* in the above list is unstable and so it is not possible to suspend a body in six degrees of freedom by this method. In particular, if permanent magnets alone are used to suspend a body, there will be at least one direction of motion in unstable equilibrium.

Technique *(ii)* provides very weak repulsion forces for materials such as bismuth [3] and is therefore of limited interest.

The well-known Meissner effect which allows a magnet to be stably levitated over a superconducting surface *(iii)* has shown interest as a possible magnetic bearing with the recent introduction of high-$T_c$ materials.

Technique *(iv)* has been used in gyroscopes and is proposed for use in high-speed Maglev trains.

A single example of technique *(v)* was cited: a thin rod undergoing zone refinement in an axial furnace was prevented from sagging by placement of the furnace in a magnetic field and running a current through the wire [4]. The method is stabilized by surface tension effects in the nearly molten rod.

Techniques *(vi)* and *(vii)* use eddy current effects as in *(iv)* stabilized by the addition of fixed electrostatic or electromagnetic fields.

Technique *(viii)* is the principle of the magnetic bearing (discussed below).

The last technique *(ix)* in Jayawant's list is of academic interest. It is possible to create stable suspension forces in systems where $\mu > \mu_0$ in some regions and $\mu < \mu_0$ in other regions, where $\mu$ is an "effective" permeability. Small iron bodies have been suspended using this technique which also includes coils and superconductors [1].

In all of the above, only technique *(viii)*, the principle of the magnetic bearing, has been shown to be practical enough for widespread application.

## 1.2 Magnetic bearings

Magnetic bearings were extensively developed by Beams *et al.* [5] in 1946, principally used to support shafts rotating at high speeds. It has also been used to support aircraft models in wind tunnels [6], and for a 5-degree-of-freedom robot hand [7]. It has been proposed to support and direct antennas in space [8], and to isolate payloads from vibration in space [9]. Application and control of such magnetic bearings continues to be an area of active research.

The magnetic Maxwell force $F_M$ per unit area is given by

$$F_M = \frac{B^2}{2\mu_0},\qquad(1)$$

where $B$ is the magnetic flux density in the air gap and $\mu_0$ is the vacuum permeability. (Equation (1) assumes a magnetic circuit with ferromagnetic material relative permeability $\mu_r \gg 1$.)

For an electromagnet suspension system, the flux density $B$ is is proportional to the product of the current $i$ and the number of coil turns $N$, and inversely proportional to the gap length $b$: $B = Ni/b$. Thus the pulling force per unit area from each actuator on the suspended iron body, is given from (1) by:

$$F_M = \frac{1}{2\mu_0}(Ni/b)^2.\qquad(2)$$

Generally in a magnetic bearing, opposed pairs of electromagnet actuators are used to pull on the suspended ferromagnetic body. Sensors to measure the gaps $b$ associated with each actuator provide feedback to the control system to regulate currents in the electromagnets for stable operation. Note the presence of the $i^2$ nonlinearity allows only uni-directional forces and gives the current-to-force characteristic a zero slope at the origin, making control difficult without the use of auxiliary bias currents. The $1/b^2$ nonlinearity approaches infinity as the gap approaches zero, also complicating control.
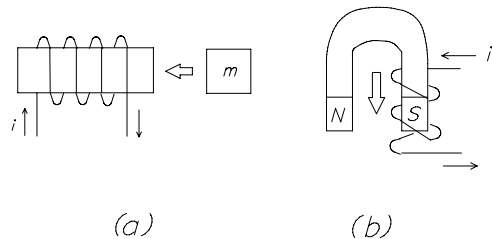


<center>(a)                  (b)</center>

Figure 1: Two Ways to Generate a Force: (a) iron mass $m$ is attracted by Maxwell electromagnetic force originating from fields induced in the iron core by current $i$ in coil, (b) coil is forced upward or downward by Lorentz electrodynamic force caused by current $i$ interacting with permanent magnetic field

This completes the Introduction. The remainder of the paper is organized as follows: Section 2 discusses the technology of using Lorentz forces for levitation, followed by Sections 3–6 which discuss possible applications of this technology. Precision assemby is discussed in Section 3, high-fidelity teleoperation is discussed in Section 4, use as a haptic computer interface is discussed in Section 5, and vibration isolation is discussed in Section 6. Conclusions are presented in Section 7.

## 2 Lorentz Levitation

In this section we introduce the notion of Lorentz levitation and contrast it with magnetic bearing suspensions based on Maxwell forces outlined above.

The magnetic Lorentz force $F_L$ per unit length of conductor is given by

$$F_L = |\mathbf{i} \times \mathbf{B}|,\qquad(3)$$

where $\mathbf{i}$ is the current vector in the conductor and $\mathbf{B}$ is the flux density vector.

The Maxwell force arises from the Maxwell's equation description of electromagnetic phenomena combined with the constitutive relation $\mathbf{B} = \mu\mathbf{H}$ describing isotropic macroscopic media. The Lorentz force, on the other hand, does not follow from Maxwell's equations, but rather from Lorentz's equation describing the force on a charged particle traveling in an electromagnetic field [10]. Figure 1 illustrates the two mechanisms for generating a force. In contrast with the Maxwell force (1), the Lorentz force (3) allows bi-directional forces with simple linear control.

The term "Lorentz levitation" introduced in this paper refers to the levitation or suspension of a body by means of the Lorentz $\mathbf{i} \times \mathbf{B}$ forces generated in current-carrying conductors immersed in magnetic fields. For stable levitation in six degrees of freedom, a minimum of six actuators and the ability to sense motion in six degrees of freedom is required.

Thus the authors propose to add a tenth technique to Jayawant's list:

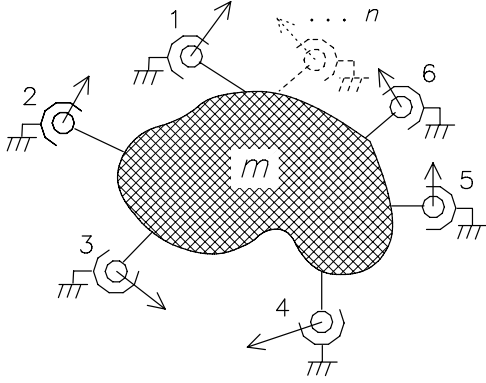*(x) levitation by forces due to controlled currents in conductors in magnetic fields.*

<center>2</center>

Figure 2: Lorentz levitation of a body of mass $m$ (schematic): Actuators $k = 1, ...6, ...n$ are attached on one side to the body and on the other side to mechanical ground in a three-dimensional arrangement. Each actuator provides a bi-directional force given by its local $\mathbf{i}_k \times \mathbf{B}_k$ vector. The position and orientation of the body $m$ is measured by sensors (not shown) to determine the $n$ currents $i_k$ according to a desired control law.

| Comparison of Methods | | |
|---|---|---|
| Attribute | Maxwell | Lorentz |
| *floating material* | ferromagnetic object | conducting coils |
| *floating mass* | high | low |
| *actuator force* | uni-directional | bi-directional |
| *force vs. current*[1] | $\sim i^2$ | $\sim i$ |
| *force vs. position* | $\sim 1/b^2$ | $\sim$ constant |
| *bias currents*[2] | required | none |
| *inductance* | high | low |
| *hysteresis & iron loss* | moderate | $\sim$ zero |
| *steady-state forces* | **large** | **small** |

Table 1: Comparison between magnetic bearing suspension and Lorentz levitation.

This new method uses the Lorentz force as in *(v)* combined with the notion of control as in *(viii)*, yet is distinctly different from either! It appears that this method was developed only recently and independently by several workers. A 1954 patent [11] describes an "electromagnetic accelerometer" developed at Hughes Aircraft, and a 1987 Draper Lab patent [12] describes a "magnetic suspension", both using Lorentz forces. A more generalized concept of Lorentz levitation was developed at the IBM T. J. Watson Research Center in the mid-1980s [13, 14]. Subsequent developments are cited in later sections of the paper.

Differences between Maxwell suspension and Lorentz levitation are highlighted in Table 1.

In all attributes but the last, Lorentz levitation appears to have distinct advantages. However, for a given total mass, the Maxwell actuator can produce up to 10 times the steady-state force of the Lorentz actuator before reaching thermal limits according to some rule-of-thumb estimates. It appears that a comprehensive, general trade-off analysis of the two types of actuators is lacking in the literature. To a large extent, the lower-force nature of the Lorentz actuator can be mitigated by using modern high-energy-product permanent magnet materials in carefully considered magnetic circuits.

## 2.1 Actuation

Referring to Figure 2, a body is levitated by at least six Lorentz actuators. Additional actuators may be used for redundancy or for additional degrees of freedom if the body is not rigid (*e.g.* has a hinge, etc.). Each actuator produces a distinct force vector while allowing full six-degree-of-freedom motion over a limited range.

Many different actuator designs are possible, with windings and magnets arranged in three-dimensional configurations. Figure 3 illustrates a generalized Lorentz actuator where a current $i$ flowing in a circuit through a controlled source C interacts with a fixed field $\mathbf{B}$ produced by a magnetic circuit M. Particular designs may have localized windings and magnets, although these elements may be distributed and more than one winding can share the field from a given magnet structure. For each actuator $k$, the current $i_k$ interacts with the local field $\mathbf{B}_k$ to produce a force

$$\mathbf{f}_k = -i_k \oint \mathbf{B}_k \times \mathbf{dl}, \qquad (4)$$

where $\mathbf{dl}$ is an element of wire in the coil and the line integral is taken over the entire coil.

Examples of Lorentz actuators include loudspeaker voice coils and rotary disk drive actuators. A specific Lorentz actuator design using four NdFeB magnets, two permeable flux return plates and a racetrack-shaped winding is discussed in [15].

For six degrees of freedom, the actuator set $\{\mathbf{f}_k, k = 1, ..., 6\}$ must be arranged so that no two actuators share a common line of action. The wrench vector $w = [f_x, f_y, f_z, \tau_x, \tau_y, \tau_z]^T$ acting on the levitated body or "flotor" is given by $w = AI$ where $I = [i_1, i_2, ..., i_6]^T$ is the vector of coil currents and $A$ is a (non-singular) $6 \times 6$ geometric transformation matrix. Whether an arbitrary force and torque can be generated on the flotor without excessively high coil currents is determined by the condition number of $A$. For example, a

---

[1] Recent hybrid magnetic bearings are quasi-linear in $i$.

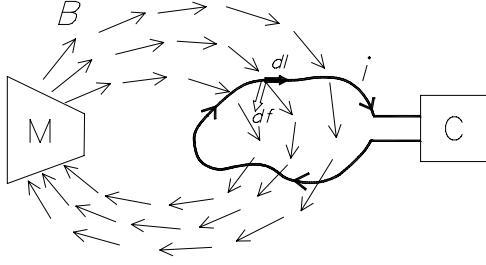[2] Not required in recent hybrid magnetic bearings.

Figure 3: Generalized Lorentz actuator: a controlled current $i$ in a coil interacts with a fixed field $\mathbf{B}$ to produce a force $\mathbf{f}$.

design using six actuators symmetrically disposed on the faces of a cube will have $\mathrm{cond}(A) = 1$ when the torque terms are normalized by the distance of the actuators from the center (radius). Less symmetric designs lead to higher values of $\mathrm{cond}(A)$.

## 2.2 Sensing

The position and orientation of the levitated body with respect to ground can be measured by several means such as capacitance– or inductance–based proximity sensors, or by optics. In systems designed by the authors, a triad of light beams fixed in the flotor and impinging on fixed position-sensing photodiodes (or *vice-versa*) was used successfully [15]. For small rotations, the position-orientation vector $p = [x, y, z, \theta_x, \theta_y, \theta_z]$ is given by $p = Sq$ where $q = [q_1, q_2, ..., q_6]^T$ is the vector of sensor measurements and $S$ is another $6 \times 6$ geometric transformation matrix.

## 2.3 Control

Control of flotor motion can be accomplished either by i) closing local feedback loops around each actuator or each sensor, or ii) globally with respect to an orthogonal $[x, y, z]$ frame $F$ imbedded in the flotor. The latter method has certain advantages, especially when the Lorentz levitator is part of a larger system operating at a higher level of control to carry out some useful function.

The flotor dynamics are essentially those of a rigid body. A small rotation angle, small angular velocity, approximately linearized model is given by[15]:

$$\ddot{\boldsymbol{\beta}} = \frac{1}{2}\dot{\boldsymbol{\omega}} = \frac{1}{2}J^{-1}\boldsymbol{\tau} \triangleq \mathbf{u}_1,$$

$$\ddot{\mathbf{r}}_T = \frac{1}{m}\mathbf{f} + \mathbf{g} - (\mathbf{r}_T - \mathbf{r}_0) \times J^{-1}\boldsymbol{\tau} \triangleq \mathbf{u}_2, \quad (5)$$

where $\boldsymbol{\omega}$ is the flotor's angular velocity, $\boldsymbol{\beta}$ is the vector part of the Euler quaternion parametrizing the orientation of the flotor relative to the stator, $\mathbf{r}_T$ is an arbitrary reference point on the flotor, $\mathbf{r}_0$ is the center of mass of the flotor and $m$ is its mass, $J$ is the flotor's inertia matrix (relative to the flotor center of mass), $\mathbf{g}$ is the gravitational acceleration vector, and $\mathbf{f}, \boldsymbol{\tau}$ are the force and torque (about the flotor's center of mass) acting on the flotor. Control efforts $\mathbf{u}_1$ and $\mathbf{u}_2$ in (5) directly effect the rotational and translational dynamics of the flotor. For rotation angles less

than $180°$, the flotor's rigid body dynamics can also be linearized *exactly* into the double integrator form $\ddot{\boldsymbol{\beta}} = \mathbf{u}_1$, $\ddot{\mathbf{r}}_T = \mathbf{u}_2$ by an exact cancellation similar to the "computed torque" method [15].

Many different control policies $\mathbf{u}_1$ and $\mathbf{u}_2$ are possible, depending on the particular application being considered. For example, a simple PD control law allowing both positioning and impedance control of the flotor can be implemented [15]:

$$\begin{aligned} \mathbf{u}_1 &= K_p(\boldsymbol{\beta}_d - \boldsymbol{\beta}) - K_v\dot{\boldsymbol{\beta}}, \\ \mathbf{u}_2 &= \tilde{K}_p(\mathbf{r}_d - \mathbf{r}_T) - \tilde{K}_v\dot{\mathbf{r}}_T, \end{aligned} \quad (6)$$

where $\mathbf{r}_d$ is the desired position of the reference point $\mathbf{r}_T$, and $\boldsymbol{\beta}_d$ describes the desired orientation of the flotor. The gains in (6) are given by:

$$\begin{aligned} K_p &\triangleq R^T \mathrm{diag}(k_{p1}, k_{p2}, k_{p3})R, \\ K_v &\triangleq R^T \mathrm{diag}(k_{v1}, k_{v2}, k_{v3})R, \\ \tilde{K}_p &\triangleq \tilde{R}^T \mathrm{diag}(\tilde{k}_{p1}, \tilde{k}_{p2}, \tilde{k}_{p3})\tilde{R}, \\ \tilde{K}_v &\triangleq \tilde{R}^T \mathrm{diag}(\tilde{k}_{v1}, \tilde{k}_{v2}, \tilde{k}_{v3})\tilde{R}. \end{aligned} \quad (7)$$

The rotation matrices $R$ and $\tilde{R}$ describe the orientations of desired control frames associated with the point $\mathbf{r}_T$, and the $k$'s are gain values.

## 3 Fine motion for precision assembly

In the automation of precision assembly tasks it is necessary for the assembly system to bring together a part or parts into correct mating relationships with the subassembly that has already been built. Accomplishing this generally requires both the ability to position the part in space, and to accommodate constraints which may be present.

Conventional robot manipulators are in general use for these tasks because of their programmability, flexibility, and large work envelopes. However, these robots suffer from several deficiencies when they are applied to precision assembly tasks with tolerances in the micrometer ($\mu$m) range.

The serial kinematic nature of their linkages results in a cantilevered machine where unavoidable flexing in the joints (and to some extent in the links) leads to loss of accuracy. Conventional drive systems using gears or belt transmissions have unavoidable backlash and static friction which further limits accuracy, motion resolution, and repeatability. Proximally located angle encoders with limited resolutions restrict the motion resolution at the distal link of the arm. Finally, the force-to-mass ratios tend to be rather small because of limitations in motor and material technologies, resulting in maximum attainable accelerations and bandwidths of a few g's and a few Hertz.

One way to circumvent this dilemma is to avoid using robots for precision assembly tasks, using instead configurations of precision linear tables, parts– and assembly–specific fixturing, optical interferometric measuring techniques, and granite or cast iron base structures to reduce vibrations. Robot arms, if used at all, are then relegated to simple parts picking or

placing; loading and unloading the specialized assembly station. These methods are reasonable when used for products of an expensive nature. However, they generally suffer from high cost and lack of flexibility when compared with general purpose robots.

Fortunately, a solution is available which effectively retains the benefits of conventional robots without its motion-problem drawbacks, while retaining the benefits of the specialized precision stage approach without its flexibility and cost drawbacks. In this solution to precision assembly, a two-stage approach is taken where a fine motion micro-robot is used in tandem with a conventional robot coarse manipulator. When combined with task-level sensing of the parts-workpiece relationship, the result is a coarse-fine manipulation system capable of delicate, precision assembly while also retaining the large workspace and flexibility benefits of the robot[16, 17, 18, 19], (see *f.* below).

Ideally, the fine-motion micro-robot should have six degrees of freedom, a reasonably low mass to minimally effect the coarse manipulator's performance, and high bandwidth. It should have much higher motion resolution than the coarse manipulator, and be free of static friction. These requirements are met in a magnetically levitated fine motion wrist described in [15].

## 3.1 The magic wrist

Figure 4 is a photograph of one version of Lorentz levitated fine-motion "magic" wrists designed by the authors [20]. As in Figure 2, a body called the "flotor" is levitated by the combined forces and torques from six Lorentz actuators, arranged at 60° intervals around a horizontal ring. Each actuator has a line of action at ±45° with respect to the vertical axis of symmetry. The permanent magnet structures of the actuators are attached to inner and outer stators which in turn are attached to the distal link of the robot arm coarse manipulator, whereas the coils of each actuator are contained in the thin, hexagonal flotor shell. The position and orientation of the flotor with respect to the stator is sensed by a triplet of optical beams projecting from the stator to a corresponding set of two-axis position-sensing photodiodes (PSDs) attached to the inside of the flotor. A set of three thin flexible ribbon cables provide power and signals to and from the flotor—the only mechanical connection between flotor and stator. The flotor has a motion range of ∼ ±5 mm in translation and ∼ ±5° in rotation, a position resolution of ∼ 1μm, and a bandwidth of ∼30 Hz.

## 3.2 Using the wrist for precision assembly

To use the wrist for assembly operations it is desirable to specify a tool frame and compliances with respect to the robot arm or wrist stator. This can be achieved by changing $\mathbf{r}_T$ in (5) and the gains and rotation matrices in (7). A different world-frame tool-point $\mathbf{r}_T$ is computed from $\mathbf{r}_T = \mathbf{r}_0 + Q^F\mathbf{r}_T$, where $Q$ is a rotation matrix describing the orientation of the flotor with respect to a world-frame and $^F\mathbf{r}_T$ is a fixed offset of the tool-point relative to the center of mass in a flotor frame. In practice, an *error integral* term is often added to (6). The magic wrist's use in preci-



Figure 4: Fine Motion Robot Wrist using Lorentz Levitation: the flotor moves in six degrees of freedom over ∼ ±5 mm in translation and ∼ ±5° in rotation.

sion assembly is described in [20], where the following modes of operation are considered.

a. *Mechanism emulation*

It is often desirable to attach a compliant mechanism as the robot end effector to accomplish accommodation tasks such as insertions. The wrist can easily be programmed to emulated a wide variety of compliant mechanisms by selecting $\mathbf{r}_T$ in (5) to be the tool point position, and setting the appropriate rotation matrices and gains in (7). Once an appropriate mechanism has been emulated, it can be used as if it were a "real" mechanism, and assembly can then be done *open-loop with respect to the task*—*i.e.*, without need for task parameter force-torque sensing or programmed decision making [20].

b. *Force control of the robot*

With isotropic high gains set in (7), the wrist can serve as a somewhat "soft" six-axis force-torque sensor in a robot force control scheme, *e.g.* [21], during assembly.

c. *Guarded moves and collision detection*

Contact with environment forces and torques can easily be detected using the wrist's high-resolution internal position/orientation sensing, and used for programmed decisions to guide the assembly operation. Because the wrist has several millimeters of free motion range, collisions can be detected in time to stop the robot motion before excessive forces are encountered.

d. *Exerting controlled forces and torques with the wrist*

The wrist can be used as a force-torque source for certain assembly operations requiring specific
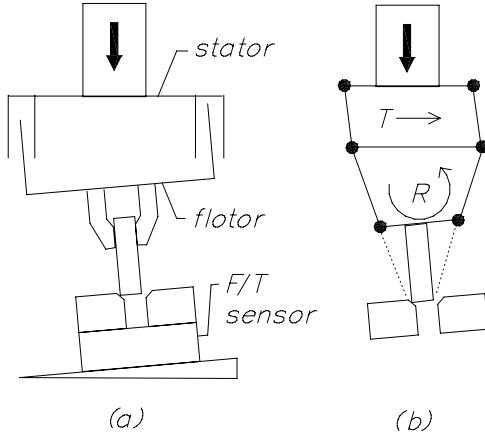
Figure 5: Peg-in-Hole Assembly using the Magic Wrist: (a) experimental arrangement showing 6-axis sensor used for measuring insertion forces and torques, (b) schematic of emulated RCC device allowing both translation and rotation of the peg about its lower end.

forces and torques to be exerted, while the robot maintains a fixed position.

e. *Compliance "in the large"*

Compliant motion over large motion ranges is achieved by programming the wrist with moderate isotropic stiffnesses, and programming the robot to track the wrist motion, *e.g.*, keep the flotor approximately centered in the stator.

f. *Coarse-fine positioning with endpoint sensing*

Many precision assembly operations are inherently *positioning* in nature and have little or nothing to do with compliance or force control. For these tasks, the coarse-fine system can be guided by external sensors that directly measure task-dependent features such as parts alignments. The high resolution and high bandwidth afforded by the wrist are very favorable for these applications.

g. *Self-correcting positioning for repetitive assembly*

Small parts positioning errors which are often met in repetitive assembly tasks can be compensated by measuring the wrist position error at parts pickup or mating, providing sufficient data to correct errors by adjusting the position of the coarse robot on subsequent cycles.

h. *Vibration during parts mating*

The wrist can be programmed to produce a complex small-amplitude six-degree-of-freedom vibration pattern to aid in parts mating.

## 3.3   Example: peg-in-hole assembly

As a precision assembly example, the magic wrist was programmed to emulate a "remote center compliance" (RCC) device (see *a*. above). Figure 5 illustrates the experimental arrangement, which included
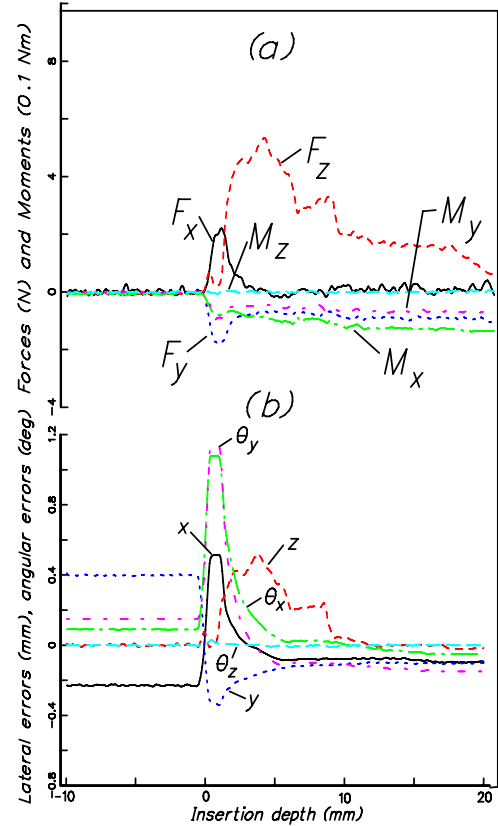


Figure 6: Peg-in-Hole Assembly Experiment Results: (a) forces and moments during peg insertion, (b) lateral and angular errors measured by magic wrist.

a JR[3] force-torque sensor used only to monitor performance [20].

Figure 6 shows results from inserting a smooth 9.538 mm diameter stainless steel peg into a stainless part with a hole having 12.6 $\mu$m clearance, and 0.5 mm, 45° chamfer. The upper set of traces (a) shows forces and moments experienced during peg insertion, and the lower set (b) shows lateral and angular errors measured by the wrist. The insertion speed in this experiment was 2 mm/s, and successful insertions were obtained when the insertion speed was increased to 100 mm/s. It can be seen that the wrist errors consistently track the measured forces (*i.e.*, verifying that the wrist can act as a force-torque sensor during assembly; see *d*. above).

It should be remarked that custom-designed *real* RCC devices will always out-perform emulated RCC devices for specific assembly situations. However, using the magic wrist for such operations in fact *enhances* the general-purpose nature of the robot: during a complicated assembly involving several different mating operations with many different parts, the system can rapidly switch between appropriately predefined end-of-arm compliant mechanisms.

# 4 High-fidelity teleoperation

By using a local "master" and a distant "slave," teleoperation extends the human manipulation ability to distant or hazardous environments. Its goal is to achieve "transparency" by mimicking the human motor and sensory functions. A rigorous definition of transparency that can be used to produce teleoperation system design goals can only be given if the teleoperation scope is narrowed to a specific task. The task considered here is the manipulation of a "tool" that can be modeled as a single rigid body.

From the mechanical interface point of view, a teleoperation system would be transparent if the operator, while observing his or her action through a vision system, could not tell whether the actual tool or the teleoperation master are maneuvered. This requires that the mechanical impedances of the master and slave be matched to that of the tool in contact with the environment and the hand, respectively, while maintaining position correspondence and stability [22, 23].

The design trade-off in achieving this goal is essentially one of gain *vs.* bandwidth, since it is difficult to design mechanisms that have a substantial motion range *and* high frequency response. The coarse-fine approach to manipulation described in Section 3 finds another useful application here. Indeed, for a limited range of motion, the teleoperation master and slave can be rigid Lorentz-levitated flotors that can be moved freely and that have similar inertial properties to those of the conventional tools operators are used to. The flotors' motion range can be enlarged by mounting their stators on conventional large motion platforms. If the forces exerted by the operator are not too large, such Lorentz-levitated flotors have position and force bandwidths that far exceed those specified in the literature as being necessary for transparency [24, 25], and therefore should be able to provide the mechanical impedance matching required for transparency.

## 4.1 Teleoperation system

A teleoperation system that uses Lorentz forces to levitate the master and the slave wrist was first presented in [26]. A newer version of the system is illustrated in Figure 7.

The slave manipulator is a conventional CRS A460 robot equipped with a Lorentz levitation wrist. The master is a Lorentz levitation wrist identical to the robot-mounted wrist. These wrists have a different actuator layout from the wrist described in Section 3—details can be found in [27]. Each of the wrists is equipped with force-torque sensors, enabling measurements of operator hand forces at the master and environment forces at the slave. Bilateral control can be achieved by a coordinated force controller that places the master and slave wrists in kinematic correspondence. If the hand and environment forces are sensed, they can be fed forward to the slave and master, respectively:

$$
\begin{aligned}
f_c &= \left(k_p + k_i \frac{1}{s} + k_v s\right)(x_m - x_s) \\
f_s &= f_h + f_c - b s x_s - \alpha f_e \\
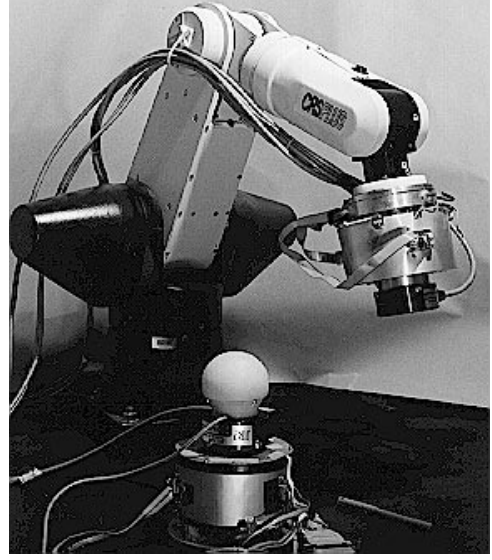f_m &= f_e - f_c \;,
\end{aligned}
\tag{8}
$$



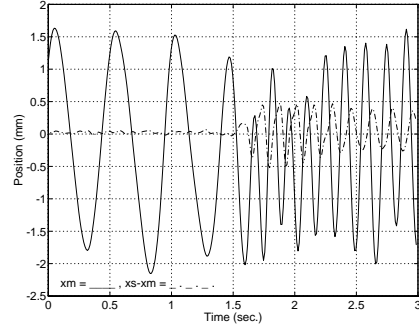Figure 7: A teleoperation system with Lorentz levitated master and slave wrist.



Figure 8: Position tracking of the master by the slave wrist: solid line is master motion; dot-dashed line is slave tracking error.

where $x_m$, $x_s$ are the master and slave locations with respect to their stators, $f_m$ and $f_s$ are the forces on the master and slave flotors, and $f_h$ and $f_e$ are the sensed hand and environment forces (flotor weight and gravity torque removal, as well as small-signal linearization are assumed in the above). The PID constants $k_p$, $k_i$, $k_s$, of the coordinating force $f_c$, and the damping terms $b$ and $\alpha$ are positive. It can be shown that if the flotors have equal masses and $b = 0$, $\alpha = 0$, this controller achieves full transparency, but its stability robustness when the slave (or master) are in contact with stiff environments is very poor. The velocity damping $b$ can be a function of the environment force or stiffness [27]. In practice, small centering PD forces are added to each of the flotors to prevent them from drifting.

Coarse positioning of the slave manipulator can be achieved by controlling the conventional robot in rate
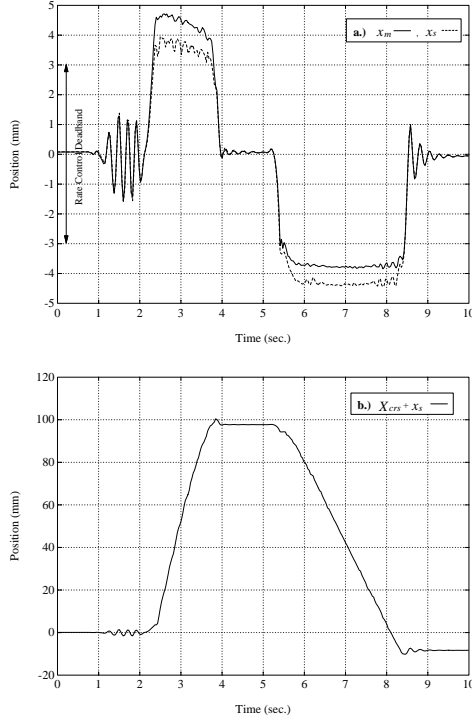
7

Figure 9: Hybrid position/rate control: (a) flotor position tracking: $x_m$ and $x_s$, (b) slave system motion: $X_R + x_s$. (The slave flotor position data, $x_s$, is measured from the stator center and is expressed in world coordinates.)



Figure 10: Exertion of forces against a stiff environment: (a) master and slave wrist positions: $x_m$ and $x_s$, (b) Hand and environment forces: $f_h$ and $-f_e$.

mode whenever the master flotor enters a peripheral region of its workspace:

$$\dot{X}_{Rd} = \begin{cases} f(\|x_m\|)\, x_m & \|x_m\| > r \\ c_v\, x_s & \text{otherwise,} \end{cases} \qquad (9)$$

where $X_{Rd}$ is the coarse robot set-point, $f(\cdot)$ is a velocity scaling function, $\|\cdot\|$ is a vector norm bounding the position-controlled workspace of the master, and $c_v$ is a small velocity constant. The continuous centering motion of the robot caused by $c_v x_s$ is necessary to allow the slave flotor to be positioned at its nominal center after it has been placed against a stiff environment [27]. Since most manipulation tasks involve a coarse positioning phase and a fine motion contact phase, the small motion range of the master does not present a problem.

## 4.2   Teleoperation results

The control and motion coordination approaches described above were implemented and shown to work well. The ability to easily position the slave flotor via decoupled coarse-fine control, and excellent kinesthetic feedback were demonstrated [27]. For example, Figure 8 shows the slave flotor tracking the master with only small errors while shaken by the operator as fast as possible (about 7 Hz).
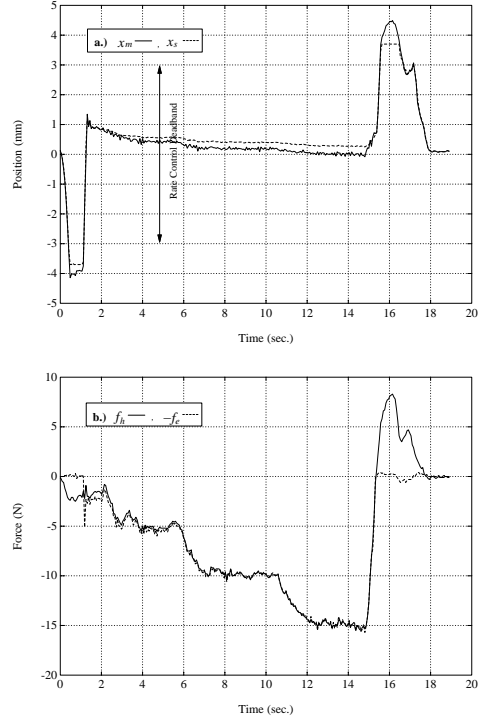
Figure 9 illustrates the hybrid position and rate control, with the master having a rate control deadband from $-3$ mm to $+3$ mm. The slave flotor position $x_s$ with respect to its own stator tracks the master flotor at all times. While the operator moves the master flotor within the rate deadband (from $t = 0$ to $t = 2$ s), the robot motion is small and due only to a slow centering term. While the master flotor is outside its position deadband, (from $t = 2$ s to $t = 4$ s), the robot velocity tracks the master position. When the operator releases the master at $t = 4$ s, both the master and the slave flotors center themselves. Backdriveability in rate mode is illustrated next, from $t = 5.2$ s onwards, when the operator pulls the slave flotor back. The master tracks the slave flotor position and the robot tracks the master in rate control. The robot velocity tracks the master position up to 1-3 Hz.

Finally, the ability to exert forces is shown in Figure 10. The operator moves the slave in rate control until the slave flotor hits the environment. The collision force pushes the master back into its position control region and the robot rate motion stops (except for the small centering motion tracking the slave flotor). After the contact, the operator attempted to exert constant forces of 5N, 10N and 15N (the sensed environment force value was displayed on a PC monitor visible to the operator). It can be seen that the environment and hand forces are essentially the same, and only a small kinematic error is present.

8

The motivation for and a discussion of (8, 9), and other experimental results can be found in [27].

## 4.3 Scaled teleoperation

The Lorentz-force approach to teleoperation can also be used when motion scaling is required, as the achievable payload-to-mass ratio does not change substantially with scaling. A miniature Lorentz levitated wrist with a flotor weighing only 30 grams has been designed for motion-scaling experiments in microsurgery [28]. For such applications, the stators of the master and slave could be in fixed relationship to each other and could be positioned by the same coarse-motion stage.

Lorentz-levitated flotors can also be used as "universal hand controllers" with force feedback, because of their high frequency response and smooth, frictionless motion. In fact, "Scaled up" application to the remote control of large hydraulic machines of the excavator type can be found in [29], and "scaled down" application to realtime control of a scanning tunneling microscope (STM) tip for "feeling" atomic-scale features on surfaces can be found in [30].

## 5 Haptic interface for virtual reality

Continual performance improvements in computer systems have enabled complex applications requiring significant interaction between the user and the computer. Examples include mechanical and electrical design, continuous and discrete simulation and optimization, and searching through large databases. In these cases users are often intimidated by lengthy panel selections and complicated commands. Clearly the lack of interaction efficiency creates a bottleneck limiting productivity.

Recently, the intelligent use of graphics, menus, and "point-and-pick" devices (e.g. mouse, tablet) has sped up many applications and attracted new users. Two relevant examples are the *Felix input device* [3] and the *Spaceball input device.* [4]

Felix has a handle that can slide on a 1 in$^2$ surface that maps the entire display area for absolute $XY$ positioning. The edges of the handle's motion range correspond to the display margins, and two of these edges contain "hot-spots" or "corners" that can be felt by the user. These locations correspond to *kinesthetically stable* places that, by appropriate programming, can be made to correspond to frequently used commands or macros [31].

The Spaceball is a spongy knob, the size of a tennis ball, attached to a six-degree-of-freedom force-torque sensor. Selected translational and rotational axes can be disabled by software control. This allows for *isometric device emulation* (e.g. "rate control" mouse emulation, by allowing only inputs that correspond to translational motion in the plane) and is useful in solid modellers for constrained rigid body motion [31].

Yet still further improvements in the user interface can be made by providing additional high-bandwidth channels carrying audio and haptic information. Equipped with actuators, input devices
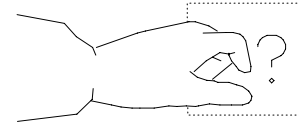
Figure 11: What to Put in the User's Hand?

can also act as output devices that provide kinesthetic feedback to the user [31, 32, 33], but there are difficulties with designing and building multi-degree-of-freedom actuated, back-driveable I/O devices. In fact, when more than three degrees of freedom are required, such I/O devices begin to resemble conventional robots—*i.e.*, serial kinematic linkages with several actuated moving parts, and are plagued by the same problems—anisotropic and high inertias, friction and low-bandwidth response.

## 5.1 Desirable characteristics

In developing a new approach to the user-computer interface, the highly-developed human hand/brain system seems a good place to start. The question is, what should be placed at the interface between the hand and the computer (Figure 11)? A fairly complete classification of input devices from a computer scientist's viewpoint can be found in [32], while a good compilation of user "wish-lists" and devices designed to cope with them can be found in [33].

First, any approach must embody good ergonomic design principles. It is desirable to provide kinesthetically stable locations for menu selection and frequently used commands. It is important for the device to be able to switch between absolute positioning (as in a data tablet) to relative positioning (as in a mouse). The ability to move intuitively in three-dimensional space or in subspaces by turning off selected degrees of freedom is highly desirable. Finally, the device should have several *actuated* degrees of freedom to provide kinesthetic feedback by force and "stiffness" control for multiple parameter adjustment and rigid body motion in simulated force fields (*e.g.* molecular "docking" [32]), or with constraints (*e.g.* geometric modelling, flight simulation). *No single computer I/O device currently satisfies this set of conditions.*

## 5.2 I/O device

In the concept presented here, the user's hand grasps and manipulates an object floating above his or her desktop. The object is positioned and oriented according to the user's will, providing a set of inputs to the computer. Alternatively, the user may exert force or torque on the floating object or some combination of forces and positioning. Most importantly, *the user can feel dynamic forces and torques on the floating object as output from the computer.* There are no motors with bearings and brushes, no gear trains with friction and backlash, and no complicated linkages between the hand and the computer to get in the way. *The floating object is levitated and controlled by the direct interactions of currents and magnetic fields* [34]. It is almost as if the user could reach his or her hand directly into the running application software!
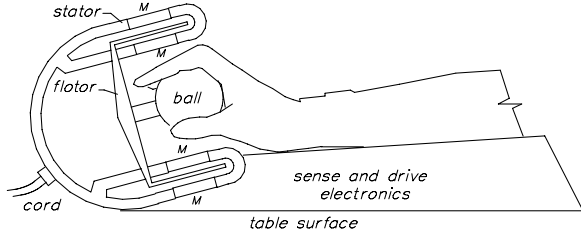
Figure 12: Possible Ergonomic Design for Lorentz Levitation I/O Device.

Figure 12 sketches a possible ergonomic design of a computer user I/O device based on Lorentz levitation. The user rests his or her hand on a cushion containing sense and drive electronics while lightly grasping a ball supported by the flotor of a Lorentz levitator. (The ball need not be spherical, could be sculpted to follow the shape of the fingers, and could incorporate one or more switches.) A motion range of $\sim$20 mm appears feasible. (If available, the authors expect that an ergonomically designed I/O device of this kind would serve well as a teleoperation master. See Section 4.) Whereas Figure 12 represents one possible design, there is a wide range of possible geometric configurations and a complete absence of critical fabrication tolerances.

## 5.3 System considerations

Figure 13 shows the system block diagram for the Lorentz I/O device. The magnetic levitation subsystem (dashed box) is a plug-in addition to a general purpose computer system. Application-specific integrated circuit (ASIC) technology would help make the subsystem compact and low in cost. A proposed software organization is illustrated in Figure 14. Both the position and orientation references and the required stiffnesses are set at a much slower rate in an asynchronous manner by the host application software through special interface routines. These interface routines, in effect, create the desired behavior, and can be thought of as emulating real mechanical devices. These emulated devices, in turn, are manipulated by the user to interact with a "virtual" environment created by the host application. For the user to be able to feel "hard" contact, for example, reasonably high stiffnesses are required. It remains to be demonstrated how well this can be achieved while simultaneously insuring stability.

An important principle is *kinesthetic correspondence* [35] between what is viewed on the display screen and how it is manipulated using the fingers or hand. It has been shown that greater user productivity occurs when the correspondence is close. This is more readily achieved in this I/O device since the mechanical properties can be programmed by the user.

## 5.4 Operation overview

Examples of how the system could be used follow below:

### Emulated Input Devices

The following is a (partial) list of emulated devices which function primarily as input devices *i.e.*, infor-
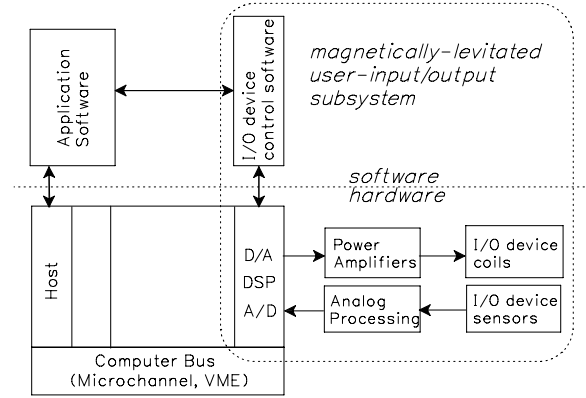


Figure 13: System Block Diagram for Lorentz I/O Device: software in the upper box runs in the general purpose workstation host; software in the lower box runs on a DSP plugged into the workstation bus.

mation mostly flows from the user's hand to the computer, with some information flowing in the opposite direction.

*a. Tablet Emulation*

The controller gains could be set to make the I/O device emulate a planar slider. The slider can be moved in the horizontal plane, while the host computer interprets its position in an $XY$ coordinate space which, for example, could control a screen pointer. Tactile indicators could be provided when the screen pointer reaches the edges of windows. For example, the user could experience a slight vertical bump whenever the pointer crossed a window boundary, giving an important cue.

*b. Multi-Plane Tablet*

The slider emulating a digitizing tablet in *a.*, above, can have *multiple planes.* By pressing or lifting harder in the $Z$ direction, the user can shift from one plane to another, with a corresponding change in the display. For example, the user could just "pop" through a series of overlapping screen windows, while feeling a "detent" position for each plane. (A two-plane demonstration with a nice "feel" was implemented in our laboratory.)

*c. Tree Traverser*

The I/O device could be programmed as in *a.*, but with multiple detents (like potential wells) corresponding to the branches of a tree. When a detent is entered, the user presses slightly, "popping through" as in *b.*, to the next level of the tree, whereupon a new set of detents is experienced, etc. This would enable the user to rapidly move through a hierarchical file system visualized as a three-dimensional tree.

*d. Joystick Emulation*

The controller gains could be set by the host computer to make the I/O device emulate a gimbal

with some restoring force and/or friction. This is accomplished by making the flotor's stiffness high, except for two rotation axes.

*e. Object Manipulation in 3-D Space*

The flotor could be programmed to "hover" in such a way that when the user displaces or rotates it, a "comfortable" restoring force and/or friction are felt. The graphical display could show a 3-D object while the user, by moving the flotor, controlled the position and orientation of the object (position control) or its velocity and angular velocity (rate control), in effect making it "fly around". This is similar to the hybrid rate-control method for teleoperation discussed in Section 4.

*f. Writing Without a Pen*

The flotor could be programmed to have a light weight and no restoring forces until it is lowered so that a virtual pen tip is in contact with a virtual piece of paper. On contact, appropriate forces and torques would be felt in the user's hand. Writing motion can then be input to the computer while appropriate software generates a synthetic left-to-right motion for each line of input.

*g. Motion-to-Text Conversion*

Motion input by the user's hand could be encoded to text by a simple scheme. For example, consider a $3 \times 3 \times 3$ cube of locations which maps into the 26 letters of the alphabet (plus null position). This could be useful for keyboardless applications or for handicapped users.

**Synthetic Output Devices**

Next is a (partial) list of devices which function primarily as output devices *i.e.*, information mostly flows from the computer to the user's hand, with some information flowing in the opposite direction.

*h. Text-to-Motion Conversion*

A string of text could easily be expressed as hand motion which could be felt and interpreted by a handicapped individual, after sufficient training.

*i. Buzzer*

Ever thought "beeps" were annoying, especially in a room full of workstations? Signals corresponding to "beeps" could briefly vibrate the I/O device's flotor, giving an inaudible non-visual cue to the user. On the other hand, higher frequency, higher amplitude signals could be fed to the flotor to operate it as a loudspeaker, if desired.

**Synthetic Input/Output Devices**

Finally is a (partial) list of devices with highly mixed input and output function *i.e.*, high realtime interaction between the computer application program and the user.
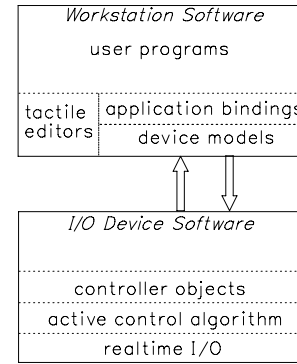


Figure 14: Possible Software Organization for Lorentz I/O Device.

*j. Terrain Mapper*

The flotor could be programmed as an $XY$ slider input device as discussed in *a.* above, but the $Z$-motion could be commanded from the application program to allow manual exploration of computed surfaces.

*k. Force Field and Constraint Sensing*

Multi-dimensional synthetic screen objects could be manually controlled (see *e.* above) while contact forces and torques were experienced by the user. Either hard contact, such as that encountered during peg-in-hole insertion, or "action at a distance," such as in molecular docking [32], could be emulated.

## 5.5 Proposed software structure

There are several ways which the software could be organized to give the user the functionality outlined in the preceding sections. We discuss here one possible approach, recalling that the user application software is running on the host machine (which can be uni- or multi-processor), and the I/O device control software is running on a DSP or DSP-like ASIC. Figure 14 shows some of the principal functional blocks of this arrangement.

Referring to the upper box of Figure 14, user programs interact with the Lorentz levitated I/O device through application bindings which relate user variables to specific actions. The user can select among many synthetic device models to use for his or her application. The device models are idealized entities which are either pre-contrived and stored in a library, or can be created. Each device model could contain a "demo mode" with suitable screen graphics for ease of understanding. A high-level "tactile editor" would allow the customization and tuning of models or building more complicated models from a simple basis set. For example, the user could select a "joystick," and while feeling around with it using his or her right hand—could adjust its axes, spring restoring forces, damping, friction, etc. by typing on the system keyboard with his or her left hand and watching a graphical representation of the values. When the joystick felt
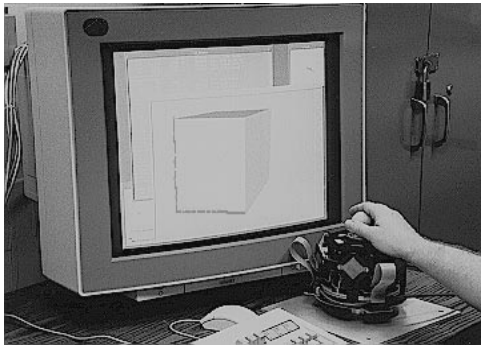
Figure 15: Experimental Setup for Lorentz I/O Device

"right" the model would be instantiated and stored. The user could create his or her personal set of "tactile icons" (tactons?) in analogy to screen "visual icons."

The lower box of Figure 14 contains software which is not directly of concern to the user. Here, device models from the workstation are mapped into controller objects on the realtime system. A controller object contains both code and data structures for operating the I/O device. A single controller object might suffice for a wide range of synthetic devices. If necessary, several controller objects can be resident, facilitating rapid switching between synthetic devices as context changes in the workstation. Only one of the controller objects is active at a given time—the "active control algorithm." Software responsible for switching the active control algorithm must also insure stability by appropriate "flaring" between gain sets.

Realtime I/O software driven by a hardware clock is running at the lowest level. Control algorithms (6) presented in Section 2 could be used.

### 5.6 Experimental setup

To evaluate some of the concepts presented in this section, the system of Figure 13 was implemented using an IBM RS/6000 workstation and Mercury DSP board. A Lorentz levitated "magic" wrist resting on the desktop served for the user interaction device substituting for the more ergonomic concept of Figure 12. A photograph of the experimental setup is shown in Figure 15.

To date, only limited software experiments have been carried out using the system mainly as an input device for manipulating solid models using a modeller developed at IBM. The most natural results have been obtained by programming the I/O device with isotropic soft restoring forces, and programming the modeller's viewer to have a small central deadband and proportional motion rate control.

In another system built at the University of British Columbia [29], a Lorentz levitated wrist was interfaced to a Silicon Graphics Iris workstation and used to interact with a simulated excavation machine, which included inertia effects and hard contact with the soil.

## 6 Vibration Isolation

Many delicate measurement or fabrication tasks in industry and science require a high degree of isolation or protection from environmental vibrational disturbances. For example, in optical holographic measurement systems, spurious vibration amplitudes of only a small fraction of a wavelength imparted to mirrors and other components can seriously degrade the measurement accuracy. In scanning tunneling microscopy, the instrument must be isolated from vibration to prevent unwanted noise in the tip-to-sample distance. Other cases occur in industry where microelectronic fabrication involves submicron dimensions. For example, in optical- and electron-beam lithography it is critical to provide protection from vibration.

Another place where vibrations must be dealt with is in space, where sensitive instruments must be isolated from the spacecraft carrying them, or in microgravity experiments where payloads must not experience any external forces. This has become a severe problem for manned space missions such as the shuttle or Freedom space station, where astronauts' activity generates unwanted vibration [36, 37].

The problem of dealing with environmental vibration is so pervasive and so critical to the success of many fields of endeavor, that a large worldwide effort has been spent on its solution. Broadly speaking, solutions can be divided into two categories: *passive* and *active*. By far the most successful solutions and the largest number have been have been of the passive type. Common examples include the pneumo-hydraulic shock absorbers on cars and the gas cylinder suspension and damping systems used for optical tables in the research environment. Less well known are active vibration isolation/cancellation systems. (We distinguish later between "isolation" and "cancellation.") Examples of active systems include servo-feedback vehicle suspensions, and vibration cancellation for optical tables, exemplified by the commercially available NRC system [38].

A special class of active vibration mechanisms includes those based on magnetic suspension. There has been much recent attention focussed in this area. For example, [37] discusses a low-frequency vibration isolation technology for microgravity space experiments which is based on magnetic bearing principles. Reference [39] discusses magnetically isolated assemblies for space application, and a one-dimensional earthbound testbed system using magnetic bearings and a force sensor in a vibration-cancelling feedback loop. Magnetic bearing vibration mounts with realtime sensing and control of electromagnetic gap flux density are proposed in [40, 41, 42].

### 6.1 Lorentz isolation in a gravity field

Lorentz levitation technology presents a new opportunity for solving the problem of vibration isolation which could be applied to many specific cases in science, industry, and space. We first consider isolation of a payload on Earth in a one-g field.

Figure 16 illustrates (in one dimension) the general principles of this approach to vibration isolation. In Figure 16(a), a mass $m$ is suspended from a platform by a spring of constant $k$, and dashpot with damping $b$. The platform experiences environmental disturbances represented by the sine-wave source referenced to "inertial ground." The spring and dashpot in (a) can be
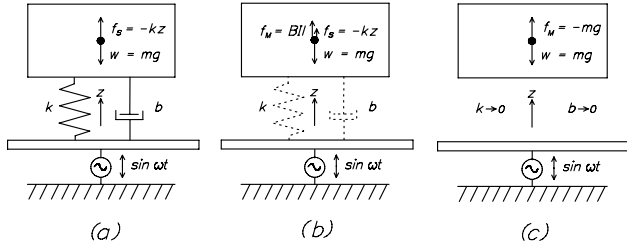
Figure 16: Vibration Isolation Principle: (a) spring and dashpot suspension—mechanical or magnetic, (b) partial replacement of suspension by magnetic force, (c) spring constant $k$ and damping $b$ approach zero as the gravity-cancelling magnetic force is increased.
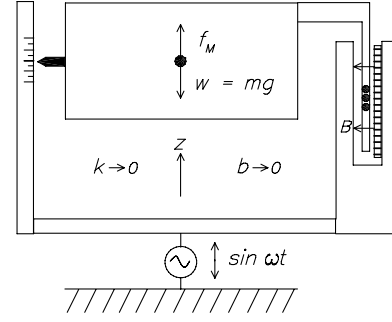


Figure 17: Vibration Isolation using Lorentz Levitation: Here, the spring and dashpot elements are synthesized by an active servo loop. Over an interval of time the value of the levitated mass is learned from the system and the spring force is gradually replaced by a constant feed-forward force, providing a high degree of isolation.

mechanical, or they can be synthesized by a magnetic force. For example, a mass may be suspended above a superconductor by magnetic flux exclusion (Meissner effect, Jayawant's method *iii*), or may be suspended below a magnet whose field strength servos it to the position $z = z_0$. In Figure 16(b), the spring and dashpot are partially offset by a Lorentz magnetic force $\mathbf{i} \times \mathbf{B}l$, or in one dimension $Bil$, where $B$ is the magnetic flux density, $i$ is the current in a conductor, and $l$ is the length of the conductor. In Figure 16(c), the Lorentz force has been adjusted to cancel gravity while $k$ and $b$ approach zero.

Figure 17 illustrates diagrammatically a Lorentz actuator and position sensor for vibration isolation in one dimension. The Lorentz actuator shown to the right of the mass $m$ provides an upward force $f_M$. This force is generated by interaction of current $i$ in conductors (solid black region) with a nearly uniform field $B$. Note that field generated by the permanent magnet (cross-hatched) is *much greater in spatial extent than the conductors*. Thus the conductors experience essentially a uniform field along a substantial distance in $z$, and also along other directions. On the left side of Figure 17 there is a sensor, represented by the pointer and scale, which continually measures the $z$-position of $m$ with respect to the vibrating platform. It is straightforward to connect the sensor readings with the actuator current to create a closed-loop system for suspending the mass above the vibrating platform. When properly operating, the servo simulates a spring inserted between mass $m$ and the vibrating platform. By inferring velocity from the sensor, or by measuring velocity directly from another sensor, a dashpot with damping $b$ can also be simulated.

The operation described to this point provides only a magnetic spring which isolates the payload through the spring-mass transfer function. Isolation making full use of the properties of Lorentz actuators requires the following adaptive procedure:

1. Initially, the platform and payload are at rest, in contact with the vibrating environment.

2. Power is turned on, and the servo loop described previously goes into operation causing the platform to levitate. The control law synthesizes a spring and dashpot, affording only partial isolation from the environment.

3. Next, an adaptive process begins. The spring constant $k$ is reduced (under analog or digital control) causing the platform to settle in response to gravity. This settling (motion in $-z$ direction) is sensed, and a compensating constant force term $f_M$ is added, tending to restore the payload to its previous position. This process continues, in a cycle, until $k$ is reduced to a very small value, and the constant force (feedforward) term is nearly equal to the weight $mg$ of the platform.

4. Now the platform is essentially isolated from the environment, since the virtual spring characterized by $k$ is exceedingly weak. The feedforward term $f_M$ can be thought of as a gravity-bucking or "anti-gravity" term. *Note that $f_M$ is essentially unaffected by vibration in $z$, since the Lorentz actuator has been contrived to operate with an essentially uniform magnetic field.*

5. Some *very small* spring constant $k$ remains to restore any gradual drift of the platform in $z$. However, at this point even further isolation can be achieved by allowing the virtual spring to respond only to the *average* displacement $\bar{z}$ in $z$ over a long time period—unlike a real spring which would respond to every cycle of the environmental vibration.

6. Remaining vibratory coupling from the environment comes from the synthetic dashpot, corresponding to back-emf generated drag on the windings from vibration of the permanent magnetic field. This emf can be measured by a separate circuit and servoed to a low value by the constant-current amplifier driving the coil. Alternatively, the coils can be wound in such a way as to cancel the generated emf.

7. (Optional). At this point, a maximum isolation from the environment has been achieved, but
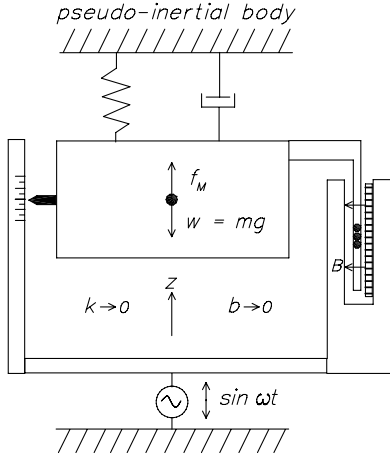
Figure 18: Optional attachment to pseudo-inertial frame.



Figure 19: Operation in space: isolation of payload from spacecraft structure.

any other disturbance to the platform from other sources—like a bug jumping up and down on it—will cause vibration to reach the payload. To reduce these effects, a (high bandwidth) servo loop can be used to attach a synthetic spring and dashpot to any convenient pseudo-inertial frame, *e.g.* a high-quality accelerometer. This condition is illustrated in Figure 18.

The above description refers to a hypothetical one-dimensional system for illustration. In reality, all six degrees of freedom must be controlled with the same strategy. This can be done with a system of at least six Lorentz actuators (cf. Figure 2 in Section 2) and with sensors that measure all six degrees of freedom. In this case, a spring *tensor* must be reduced to zero, and the gravitational *vector* must be cancelled. Note that only one of the actuators need be strong enough to cancel gravity; the other five or six actuators need only be strong enough to prevent slow drift—*e.g.*, the earth's rotation. Thus all spring constants can adaptively approach zero as feedforward terms take over, even compensating for torques caused by off-center loads. (If the payload weight or center of gravity should momentarily shift, isolation will be compromised for a short time until the adaptive control policy readjusts currents in all the actuators.)

For vibration isolation application, the Lorentz actuators must be designed to emphasize constant force operation (cf. Table 1 in Section 2). This can be done by using relatively narrow magnetic gaps with either $l_M \gg l_c$ or else $l_c \gg l_M$ where $l_M, l_c$ are the spatial extents of the magnetic field and coil windings, respectively. The actuator gaps need only be wide enough to accommodate anticipated vibration levels. One large gravity-cancelling actuator can be combined with five or six smaller stabilizing actuators. For isolation, it is highly desirable to levitate the magnet structures with the coils attached to mechanical ground (opposite of the magic wrist approach, Figure 4).

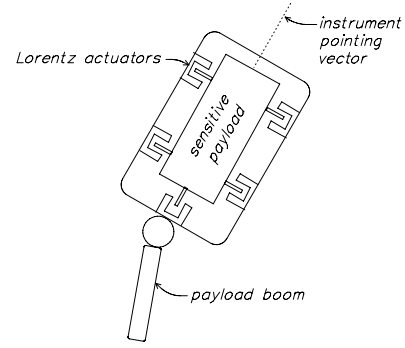Note with the adaptive algorithm sketched above, that maximum isolation occurs when the system has

"learned" the magnitude and direction of the gravity vector, and the proportional gains have approached zero. Thus it is evident that high-speed servo loops *are not required*, as no realtime sensing and cancellation of vibration is employed. This method *isolates* from, rather than *cancels*, vibration.

Calculations involving reasonable geometries (*e.g.*, 0.5 m × 0.5 m levitated platform, 45 Kg mass and payload) indicate that isolation to $4 \times 10^{-4}$ g can be reached with available power supplies and less than 300 W power expenditure.

## 6.2  Lorentz isolation in space

In space, it is possible to provide a near-zero g environment. Principal environmental disturbances arise from *i*) very low frequency ($10^{-3}$ Hz to DC) accelerations less than $10^{-6}$ g due to drag, tidal effects, and gravity gradients, *ii*) thruster activity for attitude control of $10^{-4}$ to $10^{-2}$ g, and *iii*) astronaut activity of $10^{-5}$ to $10^{-2}$ g [37].

It would appear that Lorentz magnetic levitation is a suitable technology for small-to-medium motion vibration isolation for causes *ii*) and *iii*) in near zero-gravity conditions, either in orbit or on parabolic flights, such as those executed by NASA's KC-135 aircraft. In fact, a recent patent [43] describes a Lorentz-isolated platform for space use, and SatCon Corporation has recently developed a prototype space Lorentz isolation system [44].

Unlike in one-g conditions, in near zero-g, there is no need for a large gravity-bucking actuator. Six or more actuators of modest strength could be placed in a wide variety of geometries to support a payload attached to a space vehicle (Figure 19). Operation is as follows:

1. Initially, the sensitive payload is docked while the boom is deployed and oriented in space.

2. The six-degree-of-freedom Lorentz actuators and six degree-of-freedom sensing system (not shown) within the housing take over and support the payload using synthetic springs in the manner of Figure 16.

3. The payload is then oriented with fine motion as described in Section 3 and in reference [15].

14

4. Next, the synthetic springs are gradually relaxed until a minimum current is flowing in the Lorentz actuators. The payload is now isolated from the spacecraft and its vibrations.

5. As small drifts occur, the payload position with respect to the housing can be adjusted by spacecraft thrusters (crude) or by very small currents in the actuators, causing a minimum of disturbance. The payload continues to be isolated while drift is being corrected, because of the uniform field characteristics of the Lorentz actuators.

6. (Optional). If the instrument is sighting on a remote object, such as a star, a control loop can be closed on the pointing angles, effectively connecting springs to the star direction vector. These springs can be extremely weak—just enough to prevent angular drift. Translational drift can continue to be corrected in the manner described in the previous step.

The size of the gaps required for vibration isolation depends on the disturbance acceleration amplitude and frequency. Assuming a square-wave disturbance acceleration that produces no position drift, the gap size requirement as a function of frequency is shown Figure 20 [45]. It can be seen that at $\sim 0.01$ Hz (to allow about one minute and a half for an experiment to take place), even a 1 $\mu$g acceleration level requires a motion range in excess of $\pm 10$ mm.

The gap requirements for vibration isolation on the Space Shuttle flights have been evaluated by integrating STS-40 acceleration data filtered at 0.01 Hz to eliminate orbiter rotation [45]. The resulting displacements have shown that a $\pm 10$ mm motion gap is sufficient for vibration isolation.

If the isolated experiment package is connected with the spacecraft by umbilicals, it is probably necessary to add an acceleration servo using accelerometers attached to the package (cf. Figure 18).

As an alternative to outer-space experiments and drop-towers, aircraft flights along parabolic trajectories have been executed to achieve low-cost (calculated in dollars per kilogram-second), near free-fall ($< 50$ mg) conditions of moderate duration ($< 25$ s). During such parabolic flights, equipment that is solidly attached to the aircraft is still subject to small unwanted forces, due to aircraft trajectory errors (low frequency components) and to mechanical vibrations (high frequency components).

The aircraft center-of-gravity trajectories often deviate from a perfect parabola by approximately 1-2 m over 6-7 s of free-fall [46]. Substantial pitch and roll aircraft motion compounds the error elsewhere in the aircraft. Since a single-stage large motion isolation system could not isolate a payload from aircraft vibration [46], while a Lorentz magnetic levitation isolator could not accommodate the large motion range, a coarse-fine system similar to the one discussed in Section 3 was proposed in [47]. Such a system allows controlled zero-acceleration release at the aircraft velocity and at a specific location, as well as the exertion of small centering forces on the experiment platform,
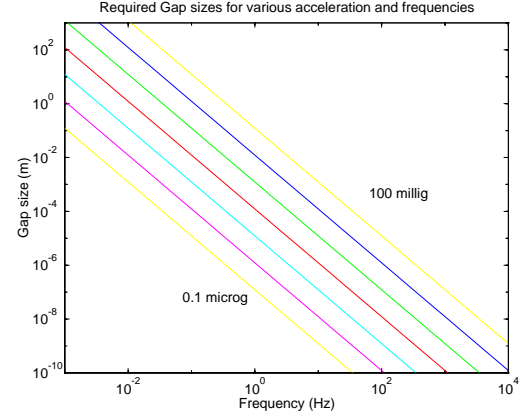


Figure 20: Required isolation gap sizes.

in effect trading acceleration levels for experiment duration.

The coarse-motion stage could be a gantry system or serial-link manipulator equipped with a spherical wrist, and would be programmed to track the isolated flotor after its release, using internally sensed flotor-stator translation and rotation offsets. Note that with fairly stringent performance limitations on the coarse motion stage performance (2 Hz bandwidth, 5 m/s$^2$ max. acceleration, 1 m/s max. velocity), typical gap requirements have been obtained from simulations using NASA KC-135 acceleration data [47]. These are of the order of $\pm 10$ mm along the aircraft pitch axis, $\pm 30$ mm along the roll axis and $\pm 40$ mm along the yaw axis. These requirements are reduced drastically as the bandwidth of the tracking platform is increased. It is possible to design a wide-gap Lorentz isolator that matches these workspace requirements. For example, the flotor could be shaped as a shell with substantial aircraft yaw-axis travel and a large face available for an experiment platform. Such a system is being developed presently in a joint project between the Canadian Space Agency and the University of British Columbia.

## 6.3 Vibration isolation experiments

Adaptive control experiments in a one-g field have been conducted in our laboratory using one of the Lorentz levitated magic wrists. Although the wrist actuators are not properly designed with the constant force *vs.* displacement property required for high-quality isolation, approximately 600-fold reductions in spring constant $k_z$ in one dimension have been achieved over adaptation times of 60 s during which only a few $\mu$m of $z$-motion occurred. These results correspond to a passband frequency $\omega_0 = 0.8$ Hz, which is quite encouraging for such an un-optimized device.

Feedback control schemes using accelerometers (inertial reference) for space and aircraft applications have been proposed and simulated, while experimental feasibility studies were carried out with a PUMA robot equipped with a Lorentz levitated wrist [47] and a single-stage large motion system equipped with the same Lorentz levitated wrist and flown on the KC-135. Flotor tracking and optimal release (at $\sim 0$ g

and 0 m/s velocity relative to the aircraft floor) have been demonstrated but vibration isolation data will be collected on a future flight.

# 7 Conclusions

The concept of Lorentz levitation of a body with full ability to control its position and orientation in space was introduced and compared with other magnetic levitation and suspension methods. Key advantages were emphasized—namely low levitated masses, force independence with position, and force linearity in current.

Four promising application areas for this technology were discussed in some detail, including use for precision assembly, teleoperation, haptic interfaces, and vibration isolation. Experimental results were reported for each of these areas, and comparisons were made with other approaches. Lorentz levitation was found to have advantages for these applications. For example, relatively low-mass floating elements are made possible since only coil structures without iron need be levitated. This fact, coupled with the relatively low-inductance of Lorentz actuator coils directly leads to high peak accelerations and high bandwidths, which in turn lead to extraordinary high performances for precision assembly, teleoperation, and haptic interfaces. On the other hand, the ability to design Lorentz actuators which exhibit near force independence with position directly leads to extraordinary high performance for vibration isolation.

There are several disadvantages associated with Lorentz levitation. Perhaps the biggest remains the relatively low force output of Lorentz actuators when compared with Maxwell actuators. Additionally, Lorentz actuators generally use air-core coils, which makes it more difficult to remove unwanted heat (especially for space applications). As with the Maxwell case, if the Lorentz actuator gap dimension is large relative to the magnet structure lateral dimensions, there will be significant fringing field losses. Thus there is a critical trade-off between actuator force and range of motion. Even with careful design and state-of-the-art magnetic materials, devices using Lorentz levitation will have motion ranges which are only a small fraction of their overall dimensions.

Lorentz levitation provides new challenges to the art of realtime control. The high bandwidths and absence of static friction tend to reduce room for error. It is likely that significant further performance improvements can be made over time with improved algorithms and implementations. It is hoped that these will lead to additional applications.

A few years ago, Lorentz levitation would not have been feasible for these applications. In the authors' view, two key elements have come together at the right time for this to happen: the introduction of new permanent magnet materials such as NdFeB with energy products of 35 MG-Oe, and recent rapid progress in computing hardware exemplified by high-speed digital signal processors. At this time, samples of NdFeB magnets with energy products up to 45 MG-Oe are becoming available, and faster DSPs are being introduced at a rapid pace, while the costs of both these technologies are continually decreasing. We eagerly look forward to future developments.

# References

[1] B. V. Jayawant, "Electromagnetic suspension and levitation techniques," *Proc. Royal Soc. Lond. A, Math. Phys. Sci.*, vol. 416, pp. 245–320, April 1988.

[2] S. Earnshaw, "On the nature of molecular forces which regulate the constitution of luminiferous ether," *Trans. Cambridge Phil. Soc.*, vol. 7, pp. 97–112, 1842.

[3] R. E. Pelrine, "Room temperature, open-loop levitation of microdevices using diamagnetic materials," in *Proc IEEE Int'l Symp. on Micro Electro Mechanical Systems*, (Napa Valley, California), pp. 34–37, February 1990.

[4] W. G. Pfann and D. W. Hagelbarger, "Electromagnetic suspension of a molten zone," *J. Appl. Phys.*, vol. 27, pp. 12–18, 1956.

[5] J. W. Beams, J. L. Young, and J. W. Moore, "The production of high centrifugal fields," *J. Appl. Physics*, vol. 17, pp. 886–890, 1946.

[6] M. H. Tuttle, D. L. Moore, and R. A. Kilgore, "Magnetic Suspension and Balance Systems: A Comprehensive, Annotated Bibliography," *NASA Technical Memorandum 4318*, pp. 1–60, August 1991.

[7] T. Higuchi, M. Tsuda, and S. Fujiwara, "Magnetic supported intelligent hand for automated precise assembly," *Proc. Int. Conf. on Industrial Electronic, Control, and Instrumentation, SPIE*, vol. 805, pp. 926–933, 1987.

[8] K. Takahara, T. Ozawa, H. Takahashi, S. Shingu, T. Ohashi, and H. Sugiura, "Development of a magnetically-suspended, tetrahedron-shaped antenna pointing system," in *Proc. NASA CP-2506, 22nd Aerospace Mechanisms Symp.*, pp. 133–147, May 4-6 1988.

[9] P. J. Wolke, "Advanced technology for active and passive vibration isolation of spaceborne payloads," in *Workshop on Vibration Isolation Technology for Microgravity Science*, (NASA Lewis Research Center, Cleveland, Ohio), September 1988.

[10] See, for example, W. D. Jackson, *Classical Electrodynamics*. New York and London: John Wiley and Sons, 1962.

[11] S. Hansen, "Electromagnetic accelerometer," *U. S. Patent No. 2,695,165*, 1954.

[12] J. R. Downer, "Magnetic suspension system," *U. S. Patent No. 4,700,094*, October 13 1987.

[13] R. L. Hollis, S. Salcudean, and A. P. Allan, "A six degree-of-freedom magnetically levitated variable compliance fine motion wrist," in *Robotics Research: 4th Int'l Symp. on Robotics Research*, (Santa Cruz, Ca.), pp. 65–73, MIT Press, August 9-14 1987.

[14] R. L. Hollis, "Six DOF magnetically levitated fine motion robot wrist with programmable compliance," *U. S. Patent No. 4,874,998*, October 1989.

[15] R. L. Hollis, S. Salcudean, and A. P. Allan, "A Six Degree-of-Freedom Magnetically Levitated Variable Compliance Fine Motion Wrist: Design, Modeling, and Control," *IEEE Transactions on Robotics and Automation*, vol. 7, pp. 320–332, June 1991.

[16] H. V. Brussel and J. Simons, "The adaptive compliance concept and its use for automatic assembly by active force feedback accomodations," in *9th Int'l Symp. on Industrial Robots*, (Washington, D.C.), pp. 167–181, 1979.

[17] R. H. Taylor, R. L. Hollis, and M. A. Lavin, "Precise manipulation with endpoint sensing," in *Proc. 2nd Int'l Symposium on Robotics Research*, (Kyoto), MIT Press, August 20-23 1984.

[18] A. Sharon and D. Hardt, "Enhancement of robot accuracy using endpoint feedback and a macro-micro manipulator system," in *Proc. American Control Conf.*, (San Diego), pp. 1836–1842, June 6-8 1984.

[19] R. H. Taylor, R. L. Hollis, and M. A. Lavin, "Precise manipulation with endpoint sensing," *IBM Jour. of Res. and Develop.*, vol. 29, pp. 363–376, July 1985.

[20] S.-R. Oh, R. L. Hollis, and S. E. Salcudean, "Precision assembly with a magnetically levitated wrist," in *IEEE Int'l Conf. on Robotics and Automation*, (Atlanta), pp. 127–134, May 1993.

[21] O. Khatib, "A unified approach for motion and force control of robot manipulators: the operational space formulation," *IEEE J. of Robotics and Automation*, vol. RA-3, no. 1, pp. 43–53, 1987.

[22] D. A. Lawrence, "Designing Teleoperator Architecture for Transparency," in *Proceedings of the IEEE International Conference on Robotics and Automation*, (Nice, France), pp. 1406–1411, May 10-15 1992.

[23] Y. Yokokohji and T. Yoshikawa, "Bilateral Control of Master-Slave Manipulators for Ideal Kinesthetic Coupling," in *Proceedings of the IEEE International Conference on Robotics and Automation*, (Nice, France), pp. 849–858, May 10-15 1992.

[24] P. Fischer, R. Daniel, and K.V.Siva, "Specification and Design of Input Devices for Teleoperation," in *Proc. IEEE Conference on Robotics and Automation*, pp. 540–545, May 1990.

[25] T. L. Brooks, "Telerobot response requirements," tech. rep., STX Robotics, 4400 Forbes Blvd., Lanham, MD 20706, March 1990.

[26] S. Salcudean, N.M. Wong, and R.L. Hollis, "A force-reflecting teleoperation system with magnetically levitated master and wrist," in *Proc. IEEE Int'l Conf. on Robotics and Automation*, (Nice, France), May 10-15, 1992.

[27] N. Wong, "Implementation of a force-reflecting telerobotic system with magnetically levitated master and wrist," Master's thesis, University of British Columbia, December 1992.

[28] S.E. Salcudean and J. Yan, "Towards a Motion Scaling System for Microsurgery," June 8-11 1993. The Third Annual IRIS-PRECARN Conference, Ottawa, Canada.

[29] N.R. Parker, S. Salcudean, and P.D. Lawrence, "Application of Force Feedback to Heavy Duty Hydraulic Machines," in *Proceedings of the IEEE International Conference on Robotics and Automation*, (Atlanta, USA), pp. 375–381, May 2-6, 1993.

[30] R. L. Hollis, S. E. Salcudean, and D. W. Abraham, "Toward a tele-nanorobotic manipulation system with atomic scale force feedback and motion resolution," in *Proc. Third IEEE Workshop on Micro Electro Mechanical Systems*, (Napa Valley, CA), pp. 115–119, Feb. 12-14 1990.

[31] T. Williams, "Input technologies extend the scope of user involvement," *Computer Design*, March 1988.

[32] M. Ouh-young, M. Pique, J. Hughes, N. Srinivasan, and F. P. B. Jr., "Using a manipulator for force display in molecular docking," in *Proc. IEEE Int'l Conf. on Robotics and Automation*, vol. 3, pp. 1824–1829, April 1988.

[33] J. Vertut and P. Coiffet, *Robot Technology, Vol. 3A: Teleoperations and Robotics: Evolution and Development*. Prentice Hall, 1986.

[34] R. L. Hollis and S. E. Salcudean, "Input/output system for computer user interface using magnetic levitation," *U. S. Patent No. 5,146,566*, September 8 1992.

[35] E. G. Britton, J. S. Lipscomb, and M. E. Pique, "Making nested rotations convenient for the user," *Computer Graphics, SIGGRAPH '78 Proc.*, vol. 12, August 23-25 1978.

[36] C. E. Rudinger, C. J. Harris, and P. C. Dolkas, "Special considerations in outfitting a space station module for scientific use," in *Proc. 16th ICES Conf. Aerospace Environmental Systems*, pp. 427–433, July 14-16 1986.

[37] C. M. Grodinsky and G. V. Brown, "Low frequency vibration isolation technology for microgravity space experiments," in *Proc. Machinery Dynamics–Applications and Vibration Control*, pp. 295–302, September 17-21 1989.

[38] Anon., "Electronic vibration isolation sytem: EVIS$^{TM}$," *NRC catalog No. 100*, pp. A–46–47, 1990.

[39] D. H. Tiszauer and E. A. Johnson, "Testing of magnetically isolated assemblies for space applications," in *Tenth Annual Rocky Mountain Guidance and Control Conf.*, pp. 319–334, Jan. 31-Feb. 4 1987.

[40] D. I. Jones and R. G. Owen, "A magnetically levitated anti-vibration mount," *IEEE Trans. on Magnetics*, vol. MAG-20, pp. 1687–1689, Sept. 1984.

[41] R. G. Owen and D. I. Jones, "Multivariable control of an active anti-vibration platform," *IEEE Trans. on Magnetics*, vol. MAG-22, pp. 523–525, Sept. 1986.

[42] R. G. Owen and D. I. Jones, "An anti-vibration platform using active suspension," in *Proc. 9th Int'l Conf. on Magnetic Technology MT-9*, (Zurich), pp. 347–350, Sept. 9-13 1985.

[43] D. G. Hoag, "Electromagnetic isolator/actuator system," *U. S. Patent No. 4,859,666*, July 18 1989.

[44] R. Fenn and B. Johnson, "A six degree of freedom lorentz force vibration isolator with nonlinear controller," in *Int'l Workshop on Vibration Isolation Technology for Microgravity Science Applications*, NASA Lewis Research Center, April 23-25 1991.

[45] N. Parker and S. E. Salcudean, "Vibration isolation with active magnetic suspension," tech. rep., The University of British Columbia, Dept. of Electrical Engineering, 2356 Main Mall, Vancouver, B.C., Canada V6T 1Z4, April 1993. Canadian Space Agency contract no. 9F008-2-0321/01SR.

[46] B.V. Tryggvason, B.Y. Stewart, H.R. Davis, and S.E. Salcudean, "Development of a Large Motion Vibration Isolation Mount for the KC-135: Summary of Flight Tests to Date," in *Spacebound '92 Workshop*, (Ottawa, Canada), May 26-28, 1992.

[47] S. Salcudean, H. Davis, C.T. Chen, D.E. Goertz, and B. Tryggvason, "Coarse-Fine Residual Gravity Cancellation System with Magnetic Levitation," in *Proceedings of the IEEE International Conference on Robotics and Automation*, (Nice, France), May 10-15, 1992.

# References

[1] B. V. Jayawant, "Electromagnetic suspension and levitation techniques," *Proc. Royal Soc. Lond. A, Math. Phys. Sci.*, vol. 416, pp. 245–320, April 1988.

[2] S. Earnshaw, "On the nature of molecular forces which regulate the constitution of luminiferous ether," *Trans. Cambridge Phil. Soc.*, vol. 7, pp. 97–112, 1842.

[3] R. E. Pelrine, "Room temperature, open-loop levitation of microdevices using diamagnetic materials," in *Proc IEEE Int'l Symp. on Micro Electro Mechanical Systems*, (Napa Valley, California), pp. 34–37, February 1990.

[4] W. G. Pfann and D. W. Hagelbarger, "Electromagnetic suspension of a molten zone," *J. Appl. Phys.*, vol. 27, pp. 12–18, 1956.

[5] J. W. Beams, J. L. Young, and J. W. Moore, "The production of high centrifugal fields," *J. Appl. Physics*, vol. 17, pp. 886–890, 1946.

[6] M. H. Tuttle, D. L. Moore, and R. A. Kilgore, "Magnetic Suspension and Balance Systems: A Comprehensive, Annotated Bibliography," *NASA Technical Memorandum 4318*, pp. 1–60, August 1991.

[7] T. Higuchi, M. Tsuda, and S. Fujiwara, "Magnetic supported intelligent hand for automated precise assembly," *Proc. Int. Conf. on Industrial Electronic, Control, and Instrumentation, SPIE*, vol. 805, pp. 926–933, 1987.

[8] K. Takahara, T. Ozawa, H. Takahashi, S. Shingu, T. Ohashi, and H. Sugiura, "Development of a magnetically-suspended, tetrahedron-shaped antenna pointing system," in *Proc. NASA CP-2506, 22nd Aerospace Mechanisms Symp.*, pp. 133–147, May 4-6 1988.

[9] P. J. Wolke, "Advanced technology for active and passive vibration isolation of spaceborne payloads," in *Workshop on Vibration Isolation Technology for Microgravity Science*, (NASA Lewis Research Center, Cleveland, Ohio), September 1988.

[10] See, for example, W. D. Jackson, *Classical Electrodynamics*. New York and London: John Wiley and Sons, 1962.

[11] S. Hansen, "Electromagnetic accelerometer," *U. S. Patent No. 2,695,165*, 1954.

[12] J. R. Downer, "Magnetic suspension system," *U. S. Patent No. 4,700,094*, October 13 1987.

[13] R. L. Hollis, S. Salcudean, and A. P. Allan, "A six degree-of-freedom magnetically levitated variable compliance fine motion wrist," in *Robotics Research: 4th Int'l Symp. on Robotics Research*, (Santa Cruz, Ca.), pp. 65–73, MIT Press, August 9-14 1987.

[14] R. L. Hollis, "Six DOF magnetically levitated fine motion robot wrist with programmable compliance," *U. S. Patent No. 4,874,998*, October 1989.

[15] R. L. Hollis, S. Salcudean, and A. P. Allan, "A Six Degree-of-Freedom Magnetically Levitated Variable Compliance Fine Motion Wrist: Design, Modeling, and Control," *IEEE Transactions on Robotics and Automation*, vol. 7, pp. 320–332, June 1991.

[16] H. V. Brussel and J. Simons, "The adaptive compliance concept and its use for automatic assembly by active force feedback accomodations," in *9th Int'l Symp. on Industrial Robots*, (Washington, D.C.), pp. 167–181, 1979.

[17] R. H. Taylor, R. L. Hollis, and M. A. Lavin, "Precise manipulation with endpoint sensing," in *Proc. 2nd Int'l Symposium on Robotics Research*, (Kyoto), MIT Press, August 20-23 1984.

[18] A. Sharon and D. Hardt, "Enhancement of robot accuracy using endpoint feedback and a macro-micro manipulator system," in *Proc. American Control Conf.*, (San Diego), pp. 1836–1842, June 6-8 1984.

[19] R. H. Taylor, R. L. Hollis, and M. A. Lavin, "Precise manipulation with endpoint sensing," *IBM Jour. of Res. and Develop.*, vol. 29, pp. 363–376, July 1985.

[20] S.-R. Oh, R. L. Hollis, and S. E. Salcudean, "Precision assembly with a magnetically levitated wrist," in *IEEE Int'l Conf. on Robotics and Automation*, (Atlanta), pp. 127–134, May 1993.

[21] O. Khatib, "A unified approach for motion and force control of robot manipulators: the operational space formulation," *IEEE J. of Robotics and Automation*, vol. RA-3, no. 1, pp. 43–53, 1987.

[22] D. A. Lawrence, "Designing Teleoperator Architecture for Transparency," in *Proceedings of the IEEE International Conference on Robotics and Automation*, (Nice, France), pp. 1406–1411, May 10-15 1992.

[23] Y. Yokokohji and T. Yoshikawa, "Bilateral Control of Master-Slave Manipulators for Ideal Kinesthetic Coupling," in *Proceedings of the IEEE International Conference on Robotics and Automation*, (Nice, France), pp. 849–858, May 10-15 1992.

[24] P. Fischer, R. Daniel, and K.V.Siva, "Specification and Design of Input Devices for Teleoperation," in *Proc. IEEE Conference on Robotics and Automation*, pp. 540–545, May 1990.

[25] T. L. Brooks, "Telerobot response requirements," tech. rep., STX Robotics, 4400 Forbes Blvd., Lanham, MD 20706, March 1990.

[26] S. Salcudean, N.M. Wong, and R.L. Hollis, "A force-reflecting teleoperation system with magnetically levitated master and wrist," in *Proc. IEEE Int'l Conf. on Robotics and Automation*, (Nice, France), May 10-15, 1992.

[27] N. Wong, "Implementation of a force-reflecting telerobotic system with magnetically levitated master and wrist," Master's thesis, University of British Columbia, December 1992.

[28] S.E. Salcudean and J. Yan, "Towards a Motion Scaling System for Microsurgery," June 8-11 1993. The Third Annual IRIS-PRECARN Conference, Ottawa, Canada.

[29] N.R. Parker, S. Salcudean, and P.D. Lawrence, "Application of Force Feedback to Heavy Duty Hydraulic Machines," in *Proceedings of the IEEE International Conference on Robotics and Automation*, (Atlanta, USA), pp. 375–381, May 2-6, 1993.

[30] R. L. Hollis, S. E. Salcudean, and D. W. Abraham, "Toward a tele-nanorobotic manipulation system with atomic scale force feedback and motion resolution," in *Proc. Third IEEE Workshop on Micro Electro Mechanical Systems*, (Napa Valley, CA), pp. 115–119, Feb. 12-14 1990.

[31] T. Williams, "Input technologies extend the scope of user involvement," *Computer Design*, March 1988.

[32] M. Ouh-young, M. Pique, J. Hughes, N. Srinivasan, and F. P. B. Jr., "Using a manipulator for force display in molecular docking," in *Proc. IEEE Int'l Conf. on Robotics and Automation*, vol. 3, pp. 1824–1829, April 1988.

[33] J. Vertut and P. Coiffet, *Robot Technology, Vol. 3A: Teleoperations and Robotics: Evolution and Development*. Prentice Hall, 1986.

[34] R. L. Hollis and S. E. Salcudean, "Input/output system for computer user interface using magnetic levitation," *U. S. Patent No. 5,146,566*, September 8 1992.

[35] E. G. Britton, J. S. Lipscomb, and M. E. Pique, "Making nested rotations convenient for the user," *Computer Graphics, SIGGRAPH '78 Proc.*, vol. 12, August 23-25 1978.

[36] C. E. Rudinger, C. J. Harris, and P. C. Dolkas, "Special considerations in outfitting a space station module for scientific use," in *Proc. 16th ICES Conf. Aerospace Environmental Systems*, pp. 427–433, July 14-16 1986.

[37] C. M. Grodinsky and G. V. Brown, "Low frequency vibration isolation technology for microgravity space experiments," in *Proc. Machinery Dynamics–Applications and Vibration Control*, pp. 295–302, September 17-21 1989.

[38] Anon., "Electronic vibration isolation sytem: EVIS$^{\text{TM}}$," *NRC catalog No. 100*, pp. A–46–47, 1990.

[39] D. H. Tiszauer and E. A. Johnson, "Testing of magnetically isolated assemblies for space applications," in *Tenth Annual Rocky Mountain Guidance and Control Conf.*, pp. 319–334, Jan. 31-Feb. 4 1987.

[40] D. I. Jones and R. G. Owen, "A magnetically levitated anti-vibration mount," *IEEE Trans. on Magnetics*, vol. MAG-20, pp. 1687–1689, Sept. 1984.

[41] R. G. Owen and D. I. Jones, "Multivariable control of an active anti-vibration platform," *IEEE Trans. on Magnetics*, vol. MAG-22, pp. 523–525, Sept. 1986.

[42] R. G. Owen and D. I. Jones, "An anti-vibration platform using active suspension," in *Proc. 9th Int'l Conf. on Magnetic Technology MT-9*, (Zurich), pp. 347–350, Sept. 9-13 1985.

[43] D. G. Hoag, "Electromagnetic isolator/actuator system," *U. S. Patent No. 4,859,666*, July 18 1989.

[44] R. Fenn and B. Johnson, "A six degree of freedom lorentz force vibration isolator with nonlinear controller," in *Int'l Workshop on Vibration Isolation Technology for Microgravity Science Applications*, NASA Lewis Research Center, April 23-25 1991.

[45] N. Parker and S. E. Salcudean, "Vibration isolation with active magnetic suspension," tech. rep., The University of British Columbia, Dept. of Electrical Engineering, 2356 Main Mall, Vancouver, B.C., Canada V6T 1Z4, April 1993. Canadian Space Agency contract no. 9F008-2-0321/01SR.

[46] B.V. Tryggvason, B.Y. Stewart, H.R. Davis, and S.E. Salcudean, "Development of a Large Motion Vibration Isolation Mount for the KC-135: Summary of Flight Tests to Date," in *Spacebound '92 Workshop*, (Ottawa, Canada), May 26-28, 1992.

[47] S. Salcudean, H. Davis, C.T. Chen, D.E. Goertz, and B. Tryggvason, "Coarse-Fine Residual Gravity Cancellation System with Magnetic Levitation," in *Proceedings of the IEEE International Conference on Robotics and Automation*, (Nice, France), May 10-15, 1992.